Available online at www.sciencedirect.com
SCIENCE DIRECT
Precambrian Research 148 (2006) 19–31
Precambrian Research
www.elsevier.com/locate/precamres

Depositional environments and an apparent age for the Geci meta-limestones: Constraints on the geological history of northern Mozambique

V.A. Melezhik [a,*], A.B. Kuznetsov [b], A.F. Fallick [c], R.A. Smith [d], I.M. Gorokhov [b], D. Jamal [e], F. Catuane [f]

[a] *Geological Survey of Norway, 7491 Trondheim, Norway*
[b] *Institute of Precambrian Geology and Geochronology, nab. Makarova, 2, 199034 St. Petersburg, Russia*
[c] *Scottish Universities Environmental Research Centre, G75 0QF East Kilbride, Glasgow, Scotland*
[d] *British Geological Survey, Murchison House, West Mains Road, Edinburgh EH9 3LA, Scotland*
[e] *Eduardo Mondlane University, PO Box 257, Maputo, Mozambique*
[f] *National Directorate for Geology, Box 217, Maputo, Mozambique*

Received 26 August 2005; received in revised form 22 February 2006; accepted 7 March 2006

Abstract

Strongly contrasting rocks were juxtaposed during the long tectonometamorphic history of the Mozambique Orogenic Belt in northern Mozambique. The latest depositional event was expressed by accumulation of marine sediments, which were subsequently mildly metamorphosed and tectonically juxtaposed with granulite facies complexes. The low-grade metasedimentary rocks comprise the Geci group which was mapped, and studied petrographically, geochemically and isotopically in order to provide constraints on the depositional environments, age and latest history of the Mozambique Orogenic Belt. The group occurs as several large, tectonically dissected, intensively sheared, folded and mylonitised, SW–NE trending lenses within Unango Complex granulite rocks. In places, primary depositional features are well preserved. The dominant rocks are calcarenites, dolarenites, calcite matrix-supported and dolostone clast-supported carbonate breccias forming beds with erosional bases, normal and reverse graded bedding, and well-developed Bouma sequences. Dolomicritic, microbial and oolitic dolostone clasts were apparently derived from the margin of a shallow-water carbonate platform and redeposited by turbidity currents on a continental slope with calcareous sedimentation. The Geci meta-carbonate rocks have low SiO_2 and Al_2O_3 contents. MgO/CaO ratios fluctuate between 0.05 and 0.70 averaging 0.15 ± 0.18 (1σ, $n = 111$). Acid-soluble constituents have moderate concentrations of Fe (777 ± 310 ppm), Mn (131 ± 85 ppm) and Sr (566 ± 145). Mn/Sr ratios are relatively low (0.26 ± 0.19), $\delta^{13}C$ and $\delta^{18}O$ values are invariably high, with only moderate scatter: $+4.0 \pm 0.6$‰ V-PDB and 25.8 ± 0.5‰ V-SMOW, respectively. The least altered $^{87}Sr/^{86}Sr$ ratio of calcite is 0.70708, whereas dolomite is enriched in ^{87}Sr with the lowest ratio of 0.70730. The least-altered $^{87}Sr/^{86}Sr$ and $\delta^{13}C$ ratios suggest an apparent depositional age of either 595–585 or 630–625 Ma. This provides a lower age limit for juxtaposition of the low-grade Geci group rocks and granulite facies rocks of the Unango Complex.

Keywords: Mozambique; Orogenic belt; Limestone; Dolostone; Carbon; Strontium; Isotopes; Age; Glaciation

* Corresponding author. Tel.: +47 73 90 42 41; fax: +47 73 92 16 20.
E-mail address: victor.melezhik@ngu.no (V.A. Melezhik).

0301-9268/$ – see front matter © 2006 Elsevier B.V. All rights reserved.
doi:10.1016/j.precamres.2006.03.003

1. Introduction

The Mozambique Orogenic Belt in northern Mozambique (Holmes, 1951) shows a prolonged and complex history involving a series of tectonometamorphic events spanning the period 1110–550 Ma (Pinna et al., 1993; Kröner et al., 2003; Muhongo et al., 2001; Johnson et al., 2005). Reconstruction of the geological evolution of such orogenic belts requires constraints on the ages and provenances of the different tectono-stratigraphic complexes that constitute the belts. In northern Mozambique, such constraints are based on a very few radiometric ages obtained from igneous and metamorphic rocks by U–Pb, Sm–Nd and Rb–Sr methods (reviewed in Johnson et al., 2005), and resulted in development of several geodynamic concepts (Holmes, 1951; Pinna et al., 1993; Shackleton, 1996; Meert, 2003; Muhongo et al., 2001). To date, there has been no attempt to obtain depositional ages from the various supracrustal rocks, which form a lesser component in the orogenic belt. The complete lack of age constraints on sedimentation and volcanism hampers further progress in understanding the geological history of the region.

Recent work in the Scandinavian Caledonides (Melezhik et al., 2001a; Melezhik et al., 2002a,b, 2003, 2005) has shown that Sr and C isotopic data, even from high-grade marble formations, can be compared with secular variations in the isotopic compositions of Neoproterozoic and Phanerozoic seawater (see review by Melezhik et al., 2001b and references therein) to obtain an apparent depositional age. Thus, despite a number of complicating factors (Melezhik et al., 2001b, 2003), carbonate chemostratigraphy may provide the age constraints necessary for deciphering the tectonostratigraphic assembly of areas where it is difficult, if not impossible, to do so using other methods.

The purpose of this work has been to constrain the depositional environment as well the depositional age of metamorphosed limestones of the Geci group using Sr and C isotope chemostratigraphy and to provide additional constraints on the tectonostratigraphy and tectonometamorphic evolution of the Mozambique Orogenic Belt.

2. Geological background

The geology of northern Mozambique remains poorly understood. Holmes (1951) was the first who recognised a high-grade north–south trending orogenic belt, the Mozambique Belt, and assigned it to a ca. 1300 Ma orogenic event, based on very early radiometric dates.

Later, Pinna et al. (1993) concluded that the Mozambican Belt in northern Mozambique was the product of two orogenic events. They recognised the Precambrian basement composed of high-grade gneisses, granulites, migmatites and orogenic plutonic rocks which were emplaced and deformed during the 1100–850 Ma Mozambican orogeny. This orogenic belt includes limited supracrustal sequences of marine provenance (Pinna et al., 1993). A later event, tentatively constrained to 900–538 Ma old, involved the deposition of limestones, phyllites, sandstones, conglomerates and some other rocks with possible glacial affinities. These rocks comprise the Geci group (Fig. 1), which was broadly correlated with the Katangan Supergroup. They also concluded that the Geci group sedimentary rocks underwent greenschist metamorphism during the ca. 538 Ma tectonic event, which also involved thrusting of these lower-grade metasedimentary complex and their older basement.

Subsequently, Muhongo et al. (2001) and Kröner et al. (2003) constrained the peak of high-grade metamorphism in northern Mozambique to ca. 615 Ma, thus questioning the previous geotectonic models. The new radiometric dates also indicated that previous tectonostratigraphic subdivisions in northern Mozambique should be considered with caution and ought to be revised (Johnson et al., 2005).

3. The Geci group

Pinna et al. (1993) described the Geci group rocks from three separate, though spatially linked, localities (Rio Messinge, Serra Macuta and Serra Geci) within Unango Complex rocks. At Serra Macuta and Serra Geci, they reported preserved primary unconformable contacts with the basement granite. At Serra Geci, the basement rocks were described as overlain by a sequence of weakly metamorphosed boulder to fine-pebble conglomerates, varved sedimentary rocks with glacial dropstones, succeeded by limestones with intraformational carbonate breccia (Pinna et al., 1993).

3.1. Tectonostratigraphic features

The Geci group rocks that occur in Serra Geci (or Jeci) are weakly metamorphosed carbonate rocks with subordinate chlorite–muscovite schists lying as a SW–NE trending tectonic lens within the Unango Complex. A roughly parallel tectonic lens within the Unango Complex, about 12 km to the NE, comprises mainly pebbly conglomeratic rocks near Monte Nacaonda (Serra Macuta locality of Pinna et al., 1993). A third tectonic

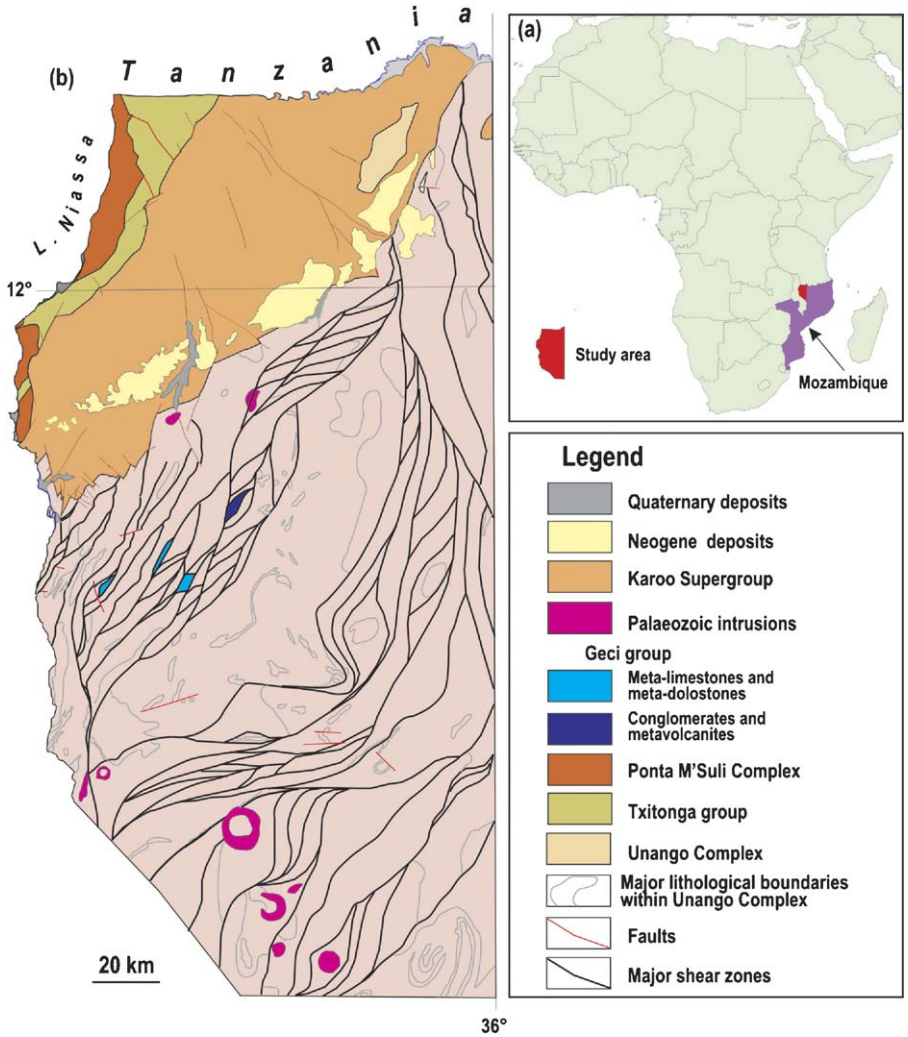

Fig. 1. Location map (a) and main geological units (b) in the study area, NW Mozambique.

lens [at ca. UTM 7011088 8573028] is exposed near the R. Chindumbe, part of the R. Messinge drainage system. It consists of weakly metamorphosed grey and white limestones with thin sandstones and grey phyllites. The low-grade Geci rocks are emplaced in orthogneiss and granofels, which have experienced granulite facies metamorphism. Although contacts between the Geci rocks and the adjacent granulite complex are not exposed, the sharp discordance in metamorphic grade implies the presence of tectonic boundaries. The Geci rocks at the margins of the lenses are generally more strongly deformed, sheared and mylonitised so the lenses representing the Geci group are assumed to be tectonically dissected units, with no primary contact with the basement rocks preserved. The mylonitised rocks are fine-grained and show thin, platy, parallel recrystallised fabric, pronounced stretching lineations, and considerable tectonic thinning. The largest lens occurs at Serra Geci, where it has a tectonostratigraphic thickness of approximately 2 km and is represented by different lithologies. The true stratigraphic thickness remains unknown due to intensive, tight, mesoscopic folding.

3.2. Sedimentological features of the Serra Geci lens

The core of the lens has been less affected by deformation, and the rocks preserve primary sedimentary structures and contacts striking ENE at 82° and dipping 70–80° SE. Three main carbonate lithologies have been recognised in the lens: (i) bedded or laminated (Fig. 2a and b), (ii) massive or graded with a clastic appearance (Fig. 2c–e) and (iii) sedimentary breccia (Fig. 2f).

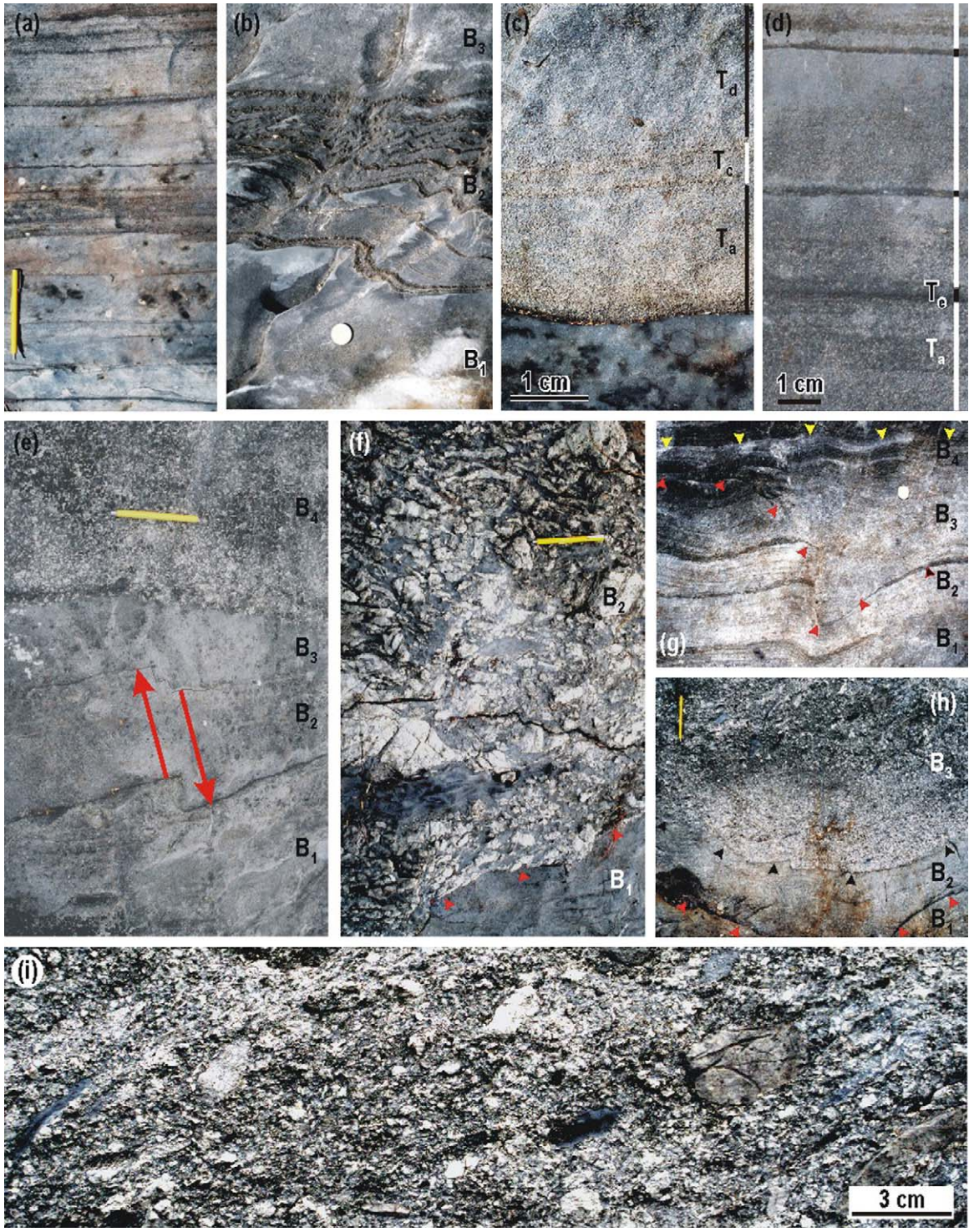

Fig. 2. Sedimentological features of the Geci metamorphosed carbonate rocks from Serra Geci. (a) Bedded unit composed of alternating thick, pale grey meta-limestone beds and dark grey, silt-rich beds. Pencil −12 cm. UTM 736356 8576736; (b) rhythmically bedded meta-limestone unit (B_2) sandwiched between two fine-grained, meta-limestone beds with massive appearance (B_1 and B_3). Coin −2 cm in diameter. UTM 736356 8576736; (c) pale grey meta-dolarenite overlying darker, fine-grained meta-limestone; the meta-dolarenite shows a Bouma sequence consisting of T_a (graded), T_c (cross-bedded) and T_d (massive) units. UTM 736587 8576692; (d) three two-unit Bouma sequences each starting with thick T_a unit of graded dolarenite and ending with thin, fine-grained, silt-rich T_e unit. UTM 736538 8576688; (e) three grey, fine-grained meta-limestone

The bedded and laminated carbonate rocks are the dominant lithology. The bedding is very regular, and is mainly due to alternation between 1 and 30 cm thick, pale grey, medium crystalline, indistinctly laminated beds and a few millimetre-thick, dark grey, fine-grained, silt-rich beds (Fig. 2a). Some beds show rhythmic lamination (Fig. 2b).

The massive carbonate rocks with clastic fabric occur as 10–80 cm-thick bodies, which commonly grade along the strike into distinctly graded beds (Fig. 2c). Commonly, only two units can be recognised in the graded beds. The bed starts with a thick unit of graded carbonate meta-sandstone (clastic, redeposited carbonates) and ends with a thin, fine-grained, silt-rich unit (Fig. 2d). These two units appear to correspond to the T_a and T_e units of a Bouma sequence. A few beds have a cross-bedded unit T_c and massive unit T_d (Fig. 2c). Several graded beds show syn-sedimentary faulting (Fig. 2e) and folding (Fig. 2g). Many beds have an erosional base (Figs. 2f–h). Erosion channels are filled with clastic carbonates showing both normal and reverse graded bedding (Fig. 2h).

Carbonate breccias occur sporadically in several places. However, due to folding, it is not possible to infer whether there are many beds or only a few, which are tectonically repeated. The breccias have sharp, commonly erosional contacts with the underlying carbonate beds. The breccias are both matrix- (Fig. 2f) and clast-supported (Fig. 2i). Fragments, pebbles and smaller clasts are mainly of dolomite, which appears to be pale grey on weathered surfaces (Fig. 2f) and dark grey on fresh surfaces. The rocks can be categorised as dolorudites when the dolostone clasts dominate. In places, the clast composition is more diverse (Fig. 2i). The majority of the clasts are angular, and platy to poorly rounded (Figs. 2f, i). The matrix is a grey, fine-grained, carbonate material with a rather massive appearance (Fig. 2f).

3.3. Petrographic features

Staining by Alizarin-red and microscopic study suggests that the carbonate rocks described above are composed of three different components occurring in variable proportions. The first, dominant, component is finely to medium-crystalline calcite whereas the second and third components are represented by dolostone and limestone clasts (Fig. 3a). All components show variable degrees of tectonic flattening and orientation.

The limestone clasts are very rare. All were severely recrystallised, have diffuse boundaries and are composed of crystalline calcite (Fig. 3a). The dolostone clasts range in size from 0.5 mm to 20 cm. Most of the larger clasts are angular and composed of dolomicrite, whereas smaller clasts are represented by rounded to sub-angular particles of dolomicrite (Fig. 3b), crystalline dolomite and dolomicrite chips (Fig. 3c). The latter may represent ripped-off fragments of dolomitised microbial mats. This inference is supported by the fact that the abundant highly disrupted microbial dolomicritic sheets are present in many medium- to large-size clasts (Fig. 3d).

Many samples contain numerous oolites or their partially recrystallised relics. Some show concentric structures (Fig. 3e) and dolospar cores (Fig. 3f), others have radial rims and dolospar cores or micritic rims and dolospar cores, which exhibit either partial or complete calcitisation.

3.4. Depositional environment

The Serra Geci carbonate rocks have sedimentary structures which are typical of those observed in turbidity current deposits. Many beds show an erosional base suggesting that high-density, suspended, clastic material was transported over, and eroded soft non-consolidated lime mud. Although a high degree of recrystallisation has severely obliterated microstructures in the fine-grained meta-limestones, they always contain a variable proportion of dolomite clasts. Moreover, there are abundant carbonate breccias, in which dolomite clasts are emplaced in a calcite matrix (Figs. 2f). Given that only very few limestone clasts have been observed, it is very likely that the Serra Geci carbonate rocks incorporated carbonate material from two distinctly different provenances. The dolomite clasts were transported over a considerable distance whereas the meta-limestones apparently represent background sediments in which redeposited dolomite clasts were incorporated. This also implies that

beds (B_1–B_3) with vague lamination overlain by graded-bedded meta-dolarenite (B_4); white specks in the meta-dolarenite are dolostone clasts in a darker calcite matrix; B_2 shows synsedimentary faulting with displacement indicated by red arrows; pencil −12 cm. UTM 736535 8576690; (f) carbonate breccia with fragments (pale grey) emplaced in dark grey, calcite matrix; note the sharp contact (arrowed in red) with the underlying meta-limestone bed. UTM 736582 8576695; (g) erosion channel (arrowed in red) in the Bouma sequence. The channel is filled with dolarenite (B_3) and overlain by B_4 showing wavy bedding plain. Beds B_1 and B_2 exhibit synsedimentary folds, apparently caused by loading of the channel infill. UTM 736587 8576692; (h) sequence of channel infills; deeply eroded bed B_1 (erosion surface is arrowed by red) infilled with meta-dolarenite (B_2) showing normal grading whereas the younger infill (above black arrows) exhibits reverse grading; (i) dolorudite with variable composition of carbonate clasts showing platy, angular and poorly rounded shapes.

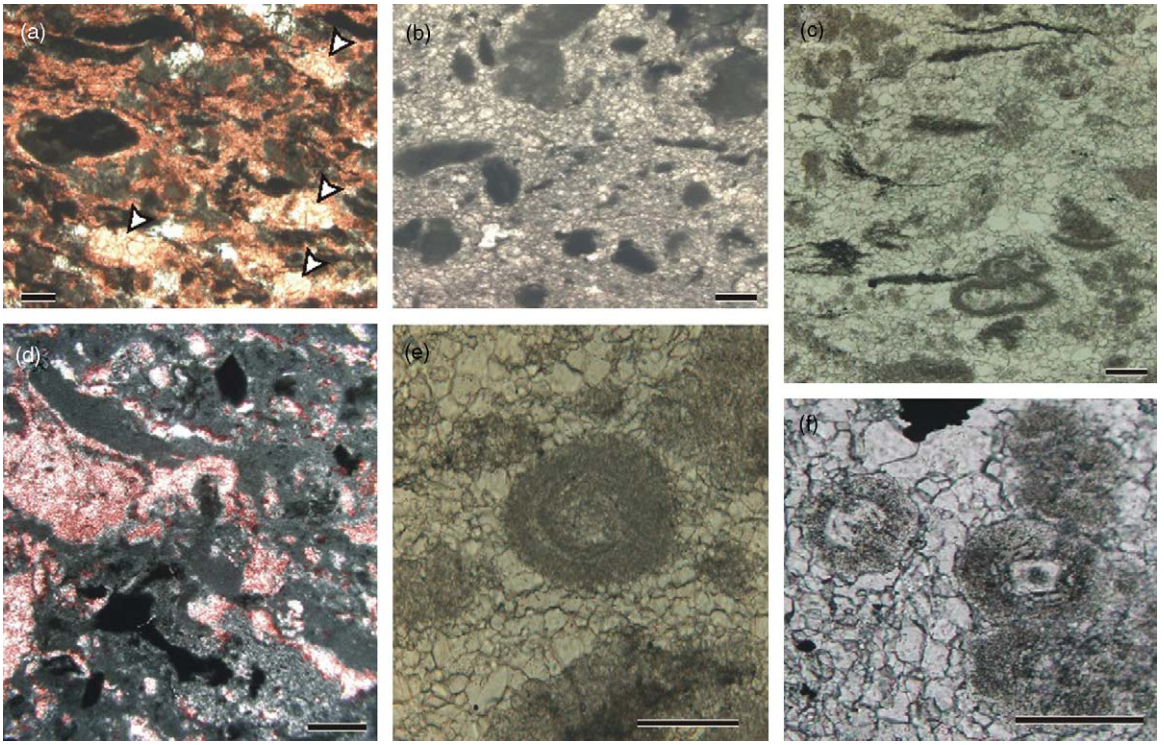

Fig. 3. Photomicrographs of polished sections demonstrating petrographic features of the Geci metamorphosed carbonate rocks from Serra Geci. (a) Alizarin-red stained polished section showing dolomicritic clasts (dark grey), recrystallised limestone clasts (pale pink indicated by arrows) in calcite matrix (pink); (b) polished section showing rounded dolomicrite clasts in a fine-grained calcite matrix; (c) dolomicrite chips, oolite and softly-deformed dolomicritic clasts in a fine-grained calcite matrix; (d) Alizarin-red stained polished section showing desiccated microbial dolomicrite (dark grey) with calcite-filled fenestrae; (e) dolomitic oolite with concentric structure emplaced in medium-grained calcite; (f) several dolomitic oolites with concentric structure and calcitised cores. Scale bar in all images −1 mm.

formation of the dolomite (either via dolomitisation or via primary dolomite precipitation) had occurred prior to redeposition of sedimentary material by turbidity currents. The presence of oolites, chips and larger fragments of microbial dolomites suggests that these materials originally formed in a shallow-water, agitated marine environment, i.e. a carbonate platform.

Clastic carbonate sequences deposited from turbidity currents are a typical feature of carbonate platform margins (Bechstädt and Boni, 1989; Grotzinger, 1989; James et al., 1989; Jiang et al., 2003). Wilson (1975) defined three types of carbonate platform margin corresponding to (1) energetically quiet, (2) moderate and (3) rough seas. All three types of environment usually produce talus on the foreslope to the carbonate platform margin. However, type 3 margins are in particular characterised by the development of widespread talus blocks, debris flows and turbidites on foreslopes and in deep-shelf settings (Wilson, 1975; Leeder, 1982). The sedimentological features of the Serra Geci carbonate rocks are most consistent with a type 3 carbonate platform margin.

The meta-limestones within the tectonic lens near the R. Chindumbe are more thoroughly deformed and recrystallised at greenschist facies metamorphic grade, although relict cross-bedding and graded bedding were observed. In general these meta-limestones are finer-grained and thinner-bedded than the Serra Geci sequence, and may represent a more distal, or energetically quieter, depositional facies.

4. Geochemistry of carbonate rocks

4.1. Analytical techniques and microsampling

Submilligram microsamples were acquired for oxygen, carbon and Rb–Sr isotope analyses using an Ulrike Medenbach microcorer, which enables core diameters from <50 μm to several millimetres to be obtained with a maximum drilling depth of 1 mm. The microsamples were cored from 150 μm thick polished sections stained by Alizarin-red.

Major and trace elements were analysed by X-ray fluorescence spectrometry at the Geological Survey of

Norway (NGU), Trondheim, using a Philips PW 1480 X-ray spectrometer. The precision (1σ) is typically around 2% of the major oxide present. Acid-soluble Fe, Ca, Mg and Mn were analysed by ICP-AES at NGU using a Thermo Jarrell Ash ICP 61 instrument. Detection limits for Fe, Mg, Ca, Mn and Sr are 5, 100, 200, 0.2 and 2 ppm, respectively. The total analytical uncertainty including element extraction (1σ) is ± 10% rel.

Oxygen and carbon isotope analyses of whole-rock and microcore samples were performed at the Scottish Universities Environmental Research Centre, Glasgow, using the phosphoric acid method of McCrea (1950) as modified by Rosenbaum and Sheppard (1986) for operation at 70 °C. Oxygen isotope data for dolomites were corrected using the fractionation factor 1.0099 recommended by Rosenbaum and Sheppard (1986). Carbon and oxygen isotope ratios in carbonate constituents of the whole-rock and microcore samples were measured on an AP 2003 mass spectrometer. Analyses were calibrated against NBS 19, and precision (1σ) for both isotope ratios is better than ± 0.2%. The carbon isotope data are reported relative to V-PDB whereas the oxygen isotope data are relative to V-SMOW.

Rb–Sr analyses of acetic acid-soluble constituent of whole-rock and microcore samples were carried out at the Institute of Precambrian Geology and Geochronology of the Russian Academy of Sciences (St. Petersburg) as specified in Gorokhov et al. (1995). The Rb and Sr concentrations were determined by isotope dilution on a MI 1320 20 cm radius, 90° sector, single-collector mass spectrometer using a triple Re filament ion source. The strontium isotopic composition was measured in static mode on a Triton multicollector thermal ionization mass spectrometer with Re-filaments. All $^{87}Sr/^{86}Sr$ ratios were normalised to a $^{86}Sr/^{88}Sr$ of 0.1194, and measurements of the NIST SRM-987 run averaged 0.710255 ± 4 ($2\sigma_{mean}$, $n = 9$). During the course of the study, the value obtained for the $^{87}Sr/^{86}Sr$ ratio of the USGS EN-1 standard was measured at 0.709191 ± 8 ($2\sigma_{mean}$, $n = 6$).

4.2. Geochemical data

Whole-rock analyses of the Serra Geci metacarbonate rocks based on new XRF analyses and previously published data (Jordan and Paulis, 1979) show relatively low SiO_2 and Al_2O_3 contents, ranging between 0.1 and 10, and 0.6 and 6 wt.%, respectively. MgO/CaO ratios fluctuate between 0.05 and 0.70, averaging around 0.15 ± 0.18 (1σ, $n = 111$), although most analyses plot within the fields of either limestone or along the dolostone–limestone-mixing line (Fig. 4). Only two

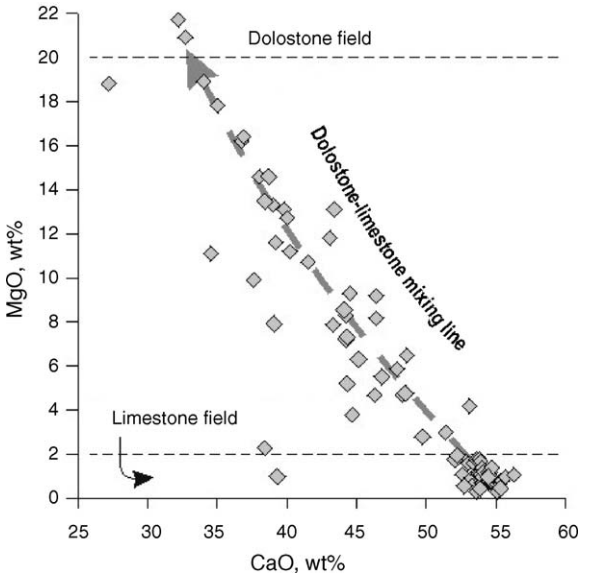

Fig. 4. MgO/CaO cross-plot of the Geci metamorphosed carbonate rocks from Serra Geci based on new analyses ($n = 17$) and previously published analytical data ($n = 94$) (Jordan and Paulis, 1979).

analyses plot in the dolostone field. Acid-soluble constituents analysed from 17 whole-rock samples (Table 1) have moderate concentrations of Fe (777 ± 310 ppm), Mn (131 ± 85 ppm) and Sr (566 ± 145). Mn/Sr ratios are relatively low (0.26 ± 0.19) but show sizeable variations (0.04–0.8), which correlate positively with the Mg/Ca ratios ($r_{Mn/Sr–Mg/Ca} = 0.55$, $n = 17$, >95.0%). The Mg/Ca ratios correlate negatively ($r = -0.74$, $n = 17$, >99.9%) with the Sr concentration (Fig. 5a). The measured $^{87}Sr/^{86}Sr$ values fluctuate between 0.70709 and 0.70736, and correlate positively with Mg/Ca ratios ($r = 0.88$, $n = 10$, >99.9%) and $\delta^{13}C$ ($r = 0.71$, $n = 10$, >95%) and negatively with the Sr concentration ($r = -0.83$, $n = 10$, >99.0%) (Fig. 5b–d). The $^{87}Sr/^{86}Sr$ ratio of microcored dolomite (0.70733) is slightly higher compared with the coeval calcite (0.70714) (Table 2). $\delta^{13}C$ and $\delta^{18}O$ values are invariably high, +4.0 ± 0.6% and 25.8 ± 0.5% ($n = 24$), respectively, and show a limited range. $\delta^{13}C$ values of microcored dolomite samples are 0.6% higher on average compared with the coeval calcite whereas $\delta^{18}O$ values are 0.6% lower.

4.3. Geochemical screening for possible post-depositional alteration

In general, the carbon isotopes are strongly buffered by the high C concentrations in carbonate mineral relative to the fluid (Banner and Hanson, 1990; Jacobsen and Kaufman, 1999) and, consequently, infiltration of

Table 1
Chemical composition of the Geci carbonate rocks

Sample (#)	SiO_2 (%)	Al_2O_3 (%)	Na_2O (%)	K_2O (%)	Mg^* (%)	Ca^* (%)	Fe^* (ppm)	Mn^* (ppm)	Sr^* (ppm)	Mn/Sr	Mg/Ca
9	2.40	0.84	–	0.18	0.99	35.6	528	58.7	679	0.09	0.03
10	2.28	2.82	–	0.13	1.65	35.2	781	59.7	623	0.10	0.05
11	2.19	0.51	–	0.15	0.24	36.7	507	69.0	509	0.14	0.006
12	0.80	0.09	–	0.04	0.58	37.4	727	61.9	655	0.09	0.02
13	3.03	0.78	–	0.21	0.30	36.5	603	63.5	627	0.10	0.008
14	0.48	0.16	–	0.08	9.15	27.2	456	76.7	248	0.3	0.34
15	2.55	0.44	–	0.15	5.21	29.9	460	219	430	0.5	0.17
16	4.15	0.80	–	0.22	4.46	30.7	1050	132	524	0.3	0.15
17	4.09	0.82	–	0.23	4.42	30.3	1080	120	516	0.2	0.15
18	4.13	1.41	0.10	0.29	3.78	31.1	1070	134	583	0.2	0.12
19	3.87	0.68	–	0.21	3.32	31.9	973	181	489	0.4	0.10
20	2.27	0.46	–	0.17	2.95	34.1	861	128	700	0.2	0.09
21	2.28	0.59	–	0.23	8.40	26.8	1360	213	493	0.4	0.31
22	2.15	0.54	–	0.18	1.18	35.8	317	288	587	0.5	0.03
23	9.75	1.76	0.32	0.48	4.86	27.2	909	313	416	0.8	0.18
24	0.96	0.23	–	0.07	0.28	38.3	384	33.2	917	0.04	0.007
25	6.75	1.30	0.24	0.36	3.15	31.0	1150	75.8	622	0.12	0.10

–: below detection limit of 0.01%; Mg^*, Ca^*, Fe^*, Mn^* and Sr^*: Mg, Ca, Fe, Mn, and Sr contents in acid-soluble constituents, determined by ICP-AES.

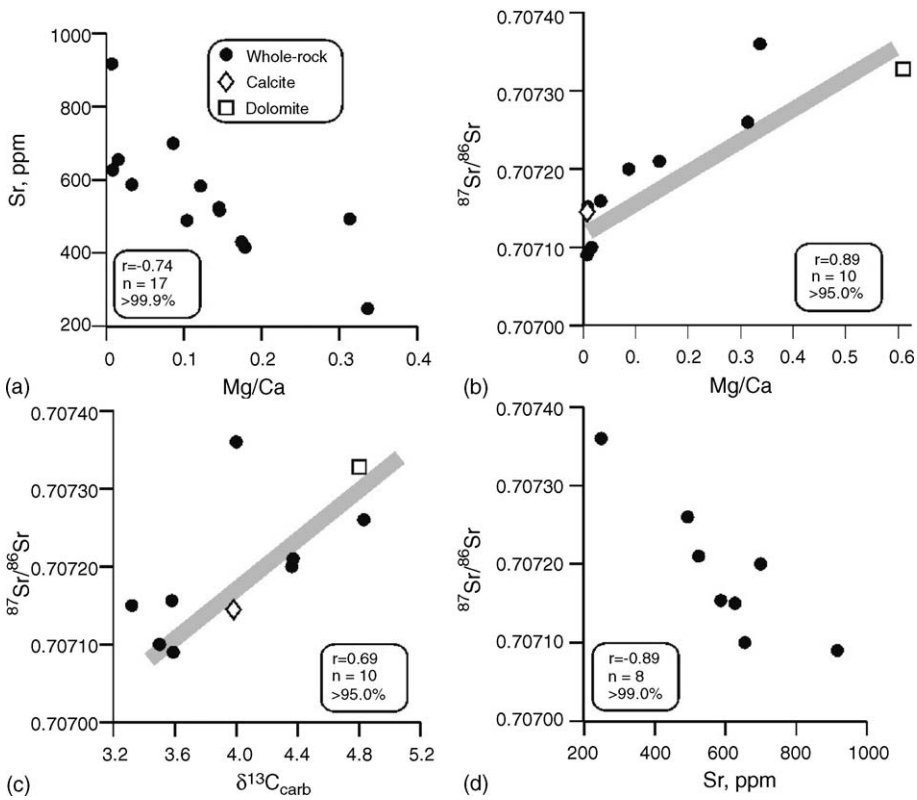

Fig. 5. Various cross-plots illustrating alteration trends and variations of geochemical parameters along calcite-dolomite mixing line (pale grey lines). Samples occurring significantly above the mixing line are considered to be altered.

Table 2
Isotopic composition, Mn/Sr and Mg/Ca ratios of the Geci carbonate rocks

Sample (#)	Mn/Sr	Mg/Ca	$\delta^{13}C$ (‰)	$\delta^{18}O$ (‰)	Rb (ppm)	Sr (ppm)	$^{87}Rb/^{86}Sr$	$^{87}Sr/^{86}Sr$ (measured)	$^{87}Sr/^{86}Sr$ (initial)	Minerals in insoluble residue
9	0.09	0.03	+3.5	26.8						
10	0.10	0.05	+3.6	25.8						
11	0.14	0.006	+2.6	25.2						
12	0.09	0.02	+3.5	25.6	0.23	653	0.0010	0.70710	0.70709	–
13	0.10	0.008	+3.3	25.2	0.26	661	0.0012	0.70715	0.70714	Qu, Ms
14	0.3	0.34	+4.0	26.4	0.23	256	0.0026	0.70736	0.70734	Grf
14 fc[a]			+3.7	26.4						
14 md[a]			+4.2	25.7						
15	0.5	0.17	+4.8	26.3						
16	0.3	0.15	+4.4	26.3	0.33	563	0.0017	0.70721	0.70720	Qu, Fsp (Ms)
16 cm[a]			+4.0	26.0						
16 dc[a]			+4.2	24.7						
17	0.2	0.15	+4.4	26.0						
18	0.2	0.12	+4.2	25.4						
19	0.4	0.10	+4.3	25.7						
20	0.2	0.09	+4.4	26.3	0.28	743	0.0011	0.70720	0.70719	Qu, Fsp, Ms
20 cm[a]		0.006[b]	+3.9	25.9	0.22	855	0.0008	0.70714	0.70713	Ms, Qu, Fsp
21	0.4	0.31	+4.8	26.3	0.30	515	0.0017	0.70726	0.70725	Ms, Qu, Fsp
21 cm[a]			+3.7	25.3						
21 md[a]		0.61[b]	+4.8	25.4	0.47	345	0.0041	0.70733	0.70730	Ms
22	0.5	0.03	+3.6	25.0	0.56	594	0.0028	0.70716	0.70714	Qu, Ms, Fsp
23	0.8	0.18	+4.4	25.3						
24	0.04	0.007	+3.6	26.3	0.35	890	0.0012	0.70709	0.70708	Qu, Ms
25	0.12	0.10	+4.2	26.0						

Abbreviated mineral names: Fsp, feldspar; Ms, muscovite; Qu, quartz; Grf, graphite.
[a] Microcore samples. The abbreviation used: cm, calcite matrix; fc, fenestreal calcite; md, microbial dolomite; dc, dolomicrite clast.
[b] Mg/Ca ratio of the dolomite microcore was assumed to be equal to stoichiometric dolomite, whereas that of the calcite microcore was considered to be equal to the lowest ratio obtained from whole-rock analyses.

externally derived fluids is likely to have a relatively greater effect on O and Sr isotopes. In the studied case, C, O and Sr isotope ratios show homogeneous distributions, which do not suggest any obvious post-depositional alteration. This is supported by the high $\delta^{18}O$ values, which are commonly more sensitive to post-depositional resetting than the carbon isotope system.

There are, however, three obvious geochemical trends associated with dolomite/calcite ratios. These include a negative correlation with Sr concentration (Fig. 5a), and the positive correlation with $^{87}Sr/^{86}Sr$ (Fig. 5b) and Mn/Sr ratios. The negative correlation can be easily attributed to mineral chemistry, i.e., the dolomite crystal lattice can admit less Sr compared to calcite. The dolomite is slightly enriched in ^{13}C compared with the calcite. The relatively high Sr concentrations in the Serra Geci meta-limestones probably provided a relatively strong buffer for the Sr isotope system although this is impossible to quantify.

Dolomite is slightly enriched in ^{87}Sr and depleted in ^{18}O with respect to calcite. Such features can be reconciled if the dolomite was a secondary phase and dolomitisation of a calcite precursor was essentially buffered by ambient seawater, slightly diluted by meteoric fluids. Alternatively, the dolomitisation might have been caused by slightly younger seawater with respect to that coeval with the calcite precursor. This would explain the slightly elevated $^{87}Sr/^{86}Sr$ ratios of the dolomite.

As the rocks studied are metamorphosed, normal petrographic screening and cathodoluminescence was of very limited use as they could only detect the alteration associated with the last geochemical transformation. Thus, although all traditional screening procedures, originally specified for non-metamorphosed or low-grade rocks (Brand and Veizer, 1980; Veizer, 1983, and later revisions; Banner and Hanson, 1990; Denison et al., 1994; Kaufman and Knoll, 1995; Azmy et al., 1998; Jacobsen and Kaufman, 1999), have been applied, the discrimination technique has been based essentially on geochemical criteria.

Conventional geochemical assessment of post-depositional alteration of carbonate is largely based on relative abundances of Mn, Fe, Rb and Sr (e.g. Brand and Veizer, 1980). Elemental ratios, such as Mn/Sr, Fe/Sr,

Ca/Sr and Rb/Sr, as well as carbon and oxygen isotopes, are widely used as geochemical criteria for detecting the least disturbed carbon, oxygen and Rb–Sr systems. Different authors, however, use not only dissimilar values of the same ratios, but also dissimilar combinations of these ratios (Asmerom et al., 1991; Derry et al., 1992; Kaufman et al., 1993; Semikhatov et al., 2002). In all cases, the choice of the elemental ratios and their values is empirical and to some extent arbitrary. The published data on non-metamorphosed limestones suggest Mn/Sr 0.065–0.02 and Mg/Ca < 0.02, whereas a significant database obtained recently from high-grade calcite marbles (Melezhik et al., 2003) suggests Mn/Sr < 0.02, Mg/Ca < 0.02.

Based on the reasoning outlined above, the least altered $^{87}Sr/^{86}Sr$ ratio of calcite from the Geci meta-limestones is tentatively considered to be 0.70708. The available data suggest a range of +3.5 to +4.8‰ as the best proxies for initial $\delta^{13}C$ of the pure calcite and dolomite phases.

5. Strontium isotopic constraints on apparent depositional age and implications for regional correlations

Strontium isotope ratios of seawater display a distinct fluctuation through time. Importantly, a long residence time of Sr in the oceans (ca. 5 million years) relative to the ocean mixing time (ca. 1500 years) (Banner, 2004) results in a very high degree of homogeneity in the oceanic Sr isotopic composition at any given time (e.g., Veizer et al., 1997, 1999). There is a gradual though irregular increase in $^{87}Sr/^{86}Sr$ ratio from ca. 850 to 500 Ma (Fig. 6), and therefore this particular time interval is well suited for indirect dating of Neoproterozoic to Early Palaeozoic carbonate rocks.

The least altered $^{87}Sr/^{86}Sr$ ratio of 0.70708 in the Serra Geci calcite is consistent with several ages within the 630–625 and 590–585 Ma time intervals if the most reliable published $^{87}Sr/^{86}Sr$ data on seawater evolution are considered (Fig. 6). Further constraint is provided by the observation that the Geci meta-limestones are directly underlain by glacial deposits in some localities (Pinna et al., 1993). Precise radiometric dates on the Neoproterozoic glacial diamictites suggest that two glaciations occurred between 635 and 580 Ma (Fig. 7). The $^{87}Sr/^{86}Sr$ ratio of 0.70708 is consistent with deposition of the Geci carbonates after the 635.5 ± 0.6 Ma Marinoan glaciation though prior to the younger (580 Ma) Gaskiers glacial event (Fig. 7). A newly constrained $\delta^{13}C$ reference curve for the 635–542 Ma time interval (Condon et al., 2005; Zhang et al., 2005) allows a further refinement. Depositional ages from 620 to 600 Ma are less probable as they are marked by highly positive $\delta^{13}C$ ratios, which are not observed in the Geci meta-limestone. The most probable ages based on the $\delta^{13}C$ calibration curve are at around 595 or between 625 and 620 Ma. Considering all the limitations involved in the isotope chemostratigraphy, the apparent depositional age of the Geci group meta-limestones is very

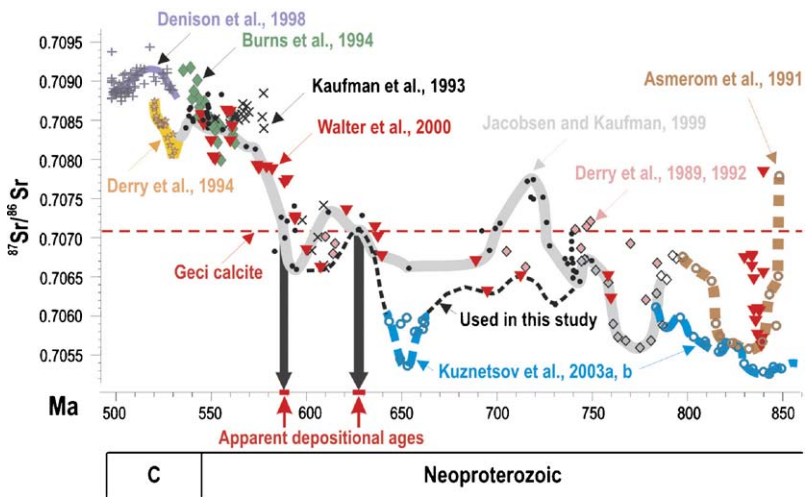

Fig. 6. Temporal trends of $^{87}Sr/^{86}Sr$ in seawater and apparent depositional ages of the Geci group carbonates (after Melezhik et al., 2001b, modified). The initial $^{87}Sr/^{86}Sr$ ratio of the least altered Geci carbonates is represented by a red horizontal dished line. Its intersection with the $^{87}Sr/^{86}Sr$-age reference curve reported in the literature gives the apparent depositional age of the studied carbonates. A vertical, arrowed-head bar indicates the most probable depositional age (see discussion in the text) (Asmerom et al., 1991; Burns et al., 1994; Denison et al., 1998; Derry et al., 1989, 1994; Jacobsen and Kaufman, 1999; Kaufman et al., 1993; Kuznetsov et al., 2003a,b; Walter et al., 2000).

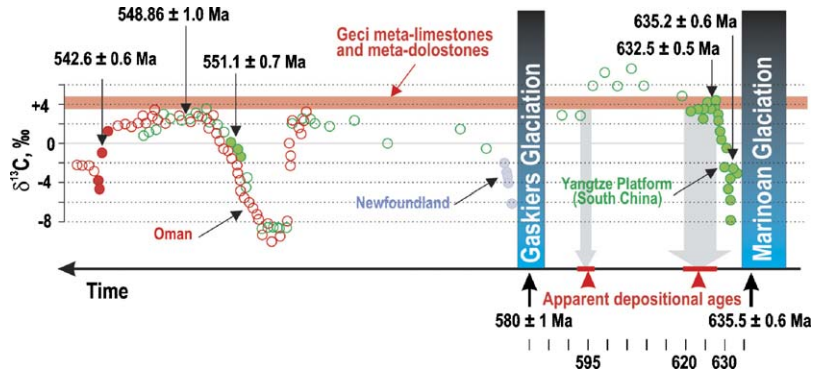

Fig. 7. Temporal trends of $\delta^{13}C$ in seawater for the 632–542 Ma time interval (modified after Condon et al., 2005) and apparent depositional ages of the Geci group carbonates. Age data are from Grotzinger et al. (1995), Martin et al. (2000), Amthor et al. (2003), Hofmann et al. (2004), Condon et al. (2005) and Zhang et al. (2005). Filled symbols are geochronologically constrained $\delta^{13}C$ values. An orange, horizontal bar shows the range of $\delta^{13}C$ values from the least altered Geci carbonates. Its intersection with $\delta^{13}C$–age reference curve gives two apparent depositional ages, which are indicated by vertical, arrowed-head bars.

likely to be between either 595 and 585 or 630 and 625 Ma.

The ages of 595–585 and 632–625 Ma have some relevance to the correlation with the Katangan Supergroup, within which two glacial events have been reported (Johnson et al., 2005) represented by a Sturtian diamictite dated at ca. 750 Ma and a younger diamictite, at the base of the Upper Kundelunga Group, estimated at 650–600 Ma. If there is a direct correlation with the Geci group (Pinna et al., 1993), the younger diamictite in the Katangan Supergroup should therefore reflect the Gaskiers (ca. 580 Ma) glaciation. If, however, the Marinoan glaciation (ca. 635 Ma) is represented in the Katangan Supergroup then the Geci group would be equivalent to a younger part of the Katangan Supergroup and the successions may not be directly correlated.

6. Conclusions

Geci group metasedimentary rocks occur in northern Mozambique as several, large, tectonically dissected, SW–NE trending lenses with Unango Complex granulite facies rocks between them. Despite intensive shearing, folding and mylonitisation, central parts of the larger Serra Geci lens preserve primary depositional features. The dominant carbonate rocks are calcarenite, dolarenites and calcite matrix-supported to dolomite clast-supported breccias. Numerous beds show erosional bases, normal and reverse graded bedding, and well-developed Bouma sequences. Clasts of mainly dolomicritic, microbial and oolitic dolostones were apparently derived from the margin of a shallow-water carbonate platform and redeposited within an unconsolidated lime mud on a continental slope. The $\delta^{13}C$ values of +3.5 to +4.8‰ and the least altered $^{87}Sr/^{86}Sr$ ratio of 0.70708 suggest two apparent depositional age intervals of either 590–585 or 630–625 Ma, which considerably narrows the duration of the latest depositional event previously constrained between 900 and 538 Ma (Pinna et al., 1993). This also provides a lower age limit for juxtaposition of the low-grade Geci group rocks and the adjacent granulite facies rocks of the Unango Complex.

Acknowledgements

This work is the part of the Mineral Resources Management Capacity Building Project, Republic of Mozambique; Component 2: Geological Infrastructure Development Programme: Geological Mapping (Lot 1) financed by the Nordic Development Fund. The C and O isotope analyses were performed at the Scottish Universities Environmental Research Centre supported by the Consortium of Scottish Universities and the Natural Environment Research Council. The Rb–Sr isotope study at the Institute of Precambrian Geology and Geochronology (St. Petersburg) was partly supported by the RFBR Projects 04-05-64915 and 05-05-65329. We are grateful to G.V. Konstantinova, N.N. Melnikov and E.P. Kutyavin for their assistance in the Rb–Sr analytical work as well as T.L. Turchenko for the XRD analyses of siliciclastic constituents of the carbonate rocks. Constructive discussions with B. Bingen, R. Boyd, I. Henderson, A. Solli and G. Viola are acknowledged with thanks. J. Karhu and an anonymous reviewer provided constructive comments on the manuscript that are greatly appreciated.

References

Amthor, J.E., Grotzinger, J.P., Schröder, S., Bowring, S.A., Ramezani, J., Martin, M.W., Matter, A., 2003. Extinction of *Cloudina* and

Namacalathus at the Precambrian–Cambrian boundary in Oman. Geology 31, 431–434.

Asmerom, Y., Jacobsen, S.B., Knoll, A.H., Butterfield, N.J., Swett, K., 1991. Strontium isotopic variations of Neoproterozoic seawater: implications for crustal evolution. Geochim. Cosmochim. Acta 55, 2883–2894.

Azmy, K., Veizer, J., Bassett, M.G., Copper, P., 1998. Oxygen and carbon isotope composition of Silurian brachiopods: implications for coeval seawater and glaciations. Geol. Soc. Am. Bull. 110, 1499–1512.

Banner, J.L., 2004. Radiogenic isotopes: systematics and applications to earth surface processes and chemical stratigraphy. Earth-Sci. Rev. 65, 141–194.

Banner, J.L., Hanson, G.N., 1990. Calculation of simultaneous isotopic and trace element variations during water–rock interaction with application to carbonate to carbonate diagenesis. Geochim. Cosmochim. Acta 54, 3123–3137.

Bechstädt, T., Boni, M., 1989. Tectonic control on the formation of a carbonate platform: the Cambrian of southwestern Sardinia. In: Crevello, P.D., Wilson, J.J., Sarq, J.F., Read, J.F. (Eds.), Controls on Carbonate Platform and Basin Development, 44. SEPM, Spec. Publ, pp. 107–122.

Brand, U., Veizer, J., 1980. Chemical diagenesis of a multicomponent carbonate system. 1. Trace elements. J. Sed. Petrol 50, 1219–1236.

Burns, S.J., Haudenschild, U., Matter, A., 1994. The strontium isotopic composition of carbonates from the late Precambrian (~560-540 Ma) Huqf Group of Oman. Chem. Geol. 111, 269–282.

Condon, D., Zhu, M., Bowring, S., Wang, W., Yang, A., Jin, Y., 2005. U–Pb ages from the Neoproterozoic Doushantuo formation, China. Science 308, 95–98.

Denison, R.E., Koepnick, R.B., Fletcher, A., Howell, M.W., Callaway, W.S., 1994. Criteria for the retention of original seawater $^{87}Sr/^{86}Sr$ in ancient shelf limestones. Chem. Geol. 112, 131–143.

Denison, R.E., Koepnick, R.B., Burke, W.H., Hetherington, E.A., 1998. Construction of the Cambrian and Ordovician seawater $^{87}Sr/^{86}Sr$ curve. Chem. Geol. 152, 325–340.

Derry, L.A., Brasier, M.D., Corfield, R.M., Rozanov, A.Y., Zhuravlev, A.Y., 1994. Sr and C isotopes in lower Cambrian carbonates from the Siberian craton: a paleoenvironmental record during the 'Cambrian explosion'. Earth Planet. Sci. Lett. 128, 671–681.

Derry, L.A., Kaufman, A.J., Jacobsen, S.B., 1992. Sedimentary cycling and environmental changes in the late Proterozoic: evidence from stable and radiogenic isotopes. Geochim. Cosmochim. Acta 56, 1317–1329.

Derry, L.A., Keto, L.S., Jacobsen, S.B., Knoll, A.H., Swett, K., 1989. Sr isotope variations in upper Proterozoic carbonates from Svalbard and East Greenland. Geochim. Cosmochim. Acta 53, 2331–2339.

Gorokhov, I.M., Semikhatov, M.A., Baskakov, A.V., Kutyavin, E.P., Mel'nikov, N.N., Sochava, A.V., Turchenko, T.L., 1995. Strontium isotope composition in Riphean Vendian and lower Cambrian carbonates. Stratig. Geol. Correl. 3, 3–33.

Grotzinger, J.P., 1989. Facies and evolution of Precambrian carbonate depositional systems: emergence of the modern platform archetype. In: Crevello, P.D., Wilson, J.L., Sarg, J.F., Read, J.F. (Eds.), Controls on Carbonate Platform and Basin Developments, 44. SEPM Spec. Publ, pp. 79–106.

Grotzinger, J.P., Bowring, S.A., Saylor, B.Z., Kaufman, A.J., 1995. Biostratigraphic and geochronologic constraints on early animal evolution. Science 270, 598–604.

Hofmann, K.H., Condon, D.J., Bowring, S.A., Crowley, J.L., 2004. U–Pb zircon date from the Neoproterozoic Ghaub formation Namibia; constraints on Marinoan glaciation. Geology 32, 817–820.

Holmes, A., 1951. The sequence of Pre-Cambrian orogenic belts in south and central Africa. In: Sandford, K.S., Blondel, F. (Eds.), The 18th International Geological Congress. Association of African Geological Surveys, London, pp. 254–269.

Jacobsen, S.B., Kaufman, A.J., 1999. The Sr C and O isotopic evolution of Neoproterozoic seawater. Chem. Geol. 161, 37–57.

James, N.P., Stevens, R.K., Barnes, C.R., Knight, I., 1989. Evolution of a lower Paleozoic continental-margin carbonate platform, northern Canadian Appalachians. In: Crevello, P.D., Wilson, J.J., Sarq, J.F., Read, J.F. (Eds.), Controls on Carbonate Platform and Basin Development, 44. SEPM, Spec. Publ, pp. 123–146.

Jiang, G., Christie-Blick, N., Kaufman, A.J., Banerjee, D.M., Rai, V., 2003. Carbonate platform growth and cyclicity at a terminal Proterozoic passive margin, Infra Krol Formation and Krol Group, lesser Himalaya India. Sedimentology 50, 921–952.

Johnson, S.P., Rivers, T., De Waele, B., 2005. A review of the Mesoproterozoic to early Palaeozoic magmatic and tectonothermal history of south-central Africa: implications for Rodinia and Gondwana. J. Geol. Soc. 162, 433–450.

Jordan, P.P., Paulis, R.V., 1979. Avaliação preliminar do jazigo de calcãrio de Malulu, Niassa. Geological Survey of Mozambique Report 61/121, 15 p. (in Portuguese).

Kaufman, A.J., Knoll, A.H., 1995. Neoproterozoic variations in the C-isotopic composition of seawater: stratigraphic and biogeochemical implications. Precambrian Res. 73, 27–49.

Kaufman, A.J., Jacobsen, S.B., Knoll, A.H., 1993. The Vendian record of Sr and C isotopic variations in seawater: implications for tectonics and paleoclimate. Earth Planet. Sci. Lett. 120, 409–430.

Kröner, A., Muhongo, S., Hegner, E., Wingate, M.T.D., 2003. Single-zircon geochronology and Nd isotopic systematics of Proterozoic high-grade rocks from the Mozambique belt of southern Tanzania (Masasi area): implications for Gondwana assembly. J. Geol. Soc. 160, 745–757.

Kuznetsov, A.B., Ovchinnikova, G.V., Gorokhov, I.M., Kaurova, O.K., Krupenin, M.T., Maslov, A.V., 2003a. Sr isotopic signature and Pb–Pb age of the Bakal formation limestones, the lower Riphean type section, the South Urals. Trans. Russian Acad. Sci. 391, 819–822.

Kuznetsov, A.B., Semikhatov, M.A., Gorokhov, I.M., Melnikov, N.N., Konstantinova, G.V., Kutyavin, E.P., 2003b. Sr isotope composition in carbonates of the Karatau Group, southern Urals, and standard curve of $^{87}Sr/^{86}Sr$ variations in the Late Riphean ocean. Stratig. Geol. Correlation 11, 415–449.

Leeder, M.R., 1982. Sedimentology. Process and Product. George Allen and Unwin Ltd., London, 344.

Martin, M.W., Grazhdankin, D.V., Bowring, S.A., Evans, D.A.D., Fedonkin, M.A., Kirschvink, J.L., 2000. Age of Neoproterozoic bilatarian body and trace fossils, White Sea Russia; implications for metazoan evolution. Science 288, 841–845.

McCrea, J.M., 1950. On the isotopic geochemistry of carbonates and a paleotemperature scale. J. Chem. Phys. 18, 849–857.

Meert, J.G., 2003. A synopsis of events related to the assembly of eastern Gondwana. Tectonophysics 362, 1–40.

Melezhik, V.A., Gorokhov, I.M., Fallick, A.E., Gjelle, S., 2001a. Strontium and carbon isotope geochemistry applied to dating of carbonate sedimentation: an example from high-grade rocks of the Norwegian Caledonides. Precambrian Res. 108, 267–292.

Melezhik, V.A., Gorokhov, I.M., Fallick, A.E., Roberts, D., Kuznetsov, A.B., Zwaan, B.K., Pokrovsky, B.G., 2002a. Isotopic stratigraphy suggests Neoproterozoic ages and Laurentian ancestry for high-

grade marbles from the north-central Norwegian Caledonides. Geol. Mag. 139, 375–393.

Melezhik, V.A., Gorokhov, I.M., Kuznetsov, A.B., Fallick, A.E., 2001b. Review article: Chemostratigraphy of Neoproterozoic carbonates: implications for 'blind dating'. Terra Nova 13, 1–11.

Melezhik, V.A., Roberts, D., Gorokhov, I.M., Fallick, A.E., Zwaan, K.B., Kuznetsov, A.B., Pokrovsky, B.G., 2002b. Isotopic evidence for a complex Neoproterozoic to Silurian rock assemblage in the north-central Norwegian Caledonides. Precambrian Res. 114, 55–86.

Melezhik, V.A., Zwaan, B.K., Motuza, G., Roberts, D., Solli, A., Fallick, A.E., Gorokhov, I.M., Kuznetsov, A.B., 2003. New insights into the geology of high-grade Caledonian marbles based on isotope chemostratigraphy. Norwegian J. Geol. 83, 209–242.

Melezhik, V.A., Roberts, D., Fallick, A.E., Gorokhov, I.M., Kuznetsov, A.B., 2005. Geochemical preservation potential of high-grade calcite marble versus dolomite marble: implication for isotope chemostratigraphy. Chem. Geol. 216, 203–224.

Muhongo, S., Kröner, A., Nemchin, A.A., 2001. Single zircon evaporation and SHRIMP ages for granulite facies rocks in the Mozambique belt of Tanzania. J. Geol. 109, 171–189.

Pinna, P., Jourde, G., Calvez, J.Y., Mroz, J.P., Marques, J.M., 1993. The Mozambique Belt in northern Mozambique: Neoproterozoic (1100–850 Ma) crustal growth and tectogenesis, and superimposed Pan-African (800–550 Ma) tectonism. Precambrian Res. 62, 1–59.

Rosenbaum, J.M., Sheppard, S.M.F., 1986. An isotopic study of siderites, dolomites and ankerites at high temperatures. Geochim. Cosmochim. Acta 50, 1147–1159.

Semikhatov, M.A., Kuznetsov, A.B., Gorokhov, I.M., Konstantinova, G.V., Melnikov, N.N., Podkovyrov, V.N., Kutyavin, E.P., 2002. Low $^{87}Sr/^{86}Sr$ ratios in seawater of the Grenville and post-Grenville time: determining factors. Stratig. Geol. Correlation 10, 1–41.

Shackleton, R.M., 1996. The final collision between East and West Gondwana. Where is it? J. Afr. Earth Sci. 23, 271–287.

Veizer, J., 1983. Trace elements and isotopes in sedimentary carbonates. In: Reeder, R.J. (Ed.), Carbonates: Mineralogy and Chemistry. Reviews in Mineralogy. Am. Mineral. Soc. 11, 265–299.

Veizer, J., Ala, D., Azmy, K., Bruckschen, P., Buhl, D., Bruhn, F., Carden, G.A.F., Diener, A., Ebneth, S., Godderis, Y., Jasper, T., Korte, C., Pawellek, F., Podlaha, O.G., Strauss, H., 1999. $^{87}Sr/^{86}Sr$, $\delta^{13}C$ and $\delta^{18}O$ evolution of Phanerozoic seawater. Chem. Geol. 161, 59–88.

Veizer, J., Buhl, D., Diener, A., Ebneth, S., Podlaha, O.G., Bruckschen, P., Jasper, T., Korte, C., Schaaf, M., Ala, D., Azmy, K., 1997. Strontium isotope stratigraphy: Potential resolution and event correlation. Palaeogeogr. Palaeoclimatol. Palaeoecol. 132, 65–77.

Walter, M.R., Veevers, J.J., Calver, C.R., Gorjan, P., Hill, A.C., 2000. Dating the 840–544 Ma Neoproterozoic interval by isotopes of strontium, carbon, and sulfur in seawater, and some interpretative models. Precambrian Res. 100, 371–433.

Wilson, J.L., 1975. Carbonate Facies in Geological History. Springer-Verlag, Berlin, p. 471.

Zhang, S., Jiang, G., Zhang, J., Song, B., Kennedy, M.J., Christie-Blick, N., 2005. U–Pb sensitive high-resolution ion microprobe ages from the Doushantuo Formation in South China: constraints on late Neoproterozoic glaciations. Geology 33, 473–476.